Physiol Genomics 41: 224–231, 2010.
First published March 2, 2010; doi:10.1152/physiolgenomics.00188.2009.

CALL FOR PAPERS | *Computational Modeling of Physiological Systems*

Metabolomic study of the LDL receptor null mouse fed a high-fat diet reveals profound perturbations in choline metabolism that are shared with ApoE null mice

Kian-Kai Cheng,[1,2] G. Martin Benson,[3] David C. Grimsditch,[4] David G. Reid,[4] Susan C. Connor,[1,4] and Julian L. Griffin[1,5,6]

[1]*Department of Biochemistry,* [5]*Institute of Metabolic Sciences,* [6]*The Cambridge Systems Biology Centre, University of Cambridge, Cambridge, United Kingdom;* [2]*Department of Bioprocess Engineering, Faculty of Chemical and Natural Resources Engineering, Universiti Teknologi Malaysia, Skudai, Johor, Malaysia;* [3]*Metabolic Disease Biology Area, Hoffmann-La Roche, Basel, Switzerland; and* [4]*Safety Assessment Division, GlaxoSmithKline, Ware, United Kingdom*

Submitted 2 November 2009; accepted in final form 27 February 2010

Cheng K-K, Benson GM, Grimsditch DC, Reid DG, Connor SC, Griffin JL. Metabolomic study of the LDL receptor null mouse fed a high-fat diet reveals profound perturbations in choline metabolism that are shared with ApoE null mice. *Physiol Genomics* 41: 224–231, 2010. First published March 2, 2010; doi:10.1152/physiolgenomics.00188.2009.—Failure to express or expression of dysfunctional low-density lipoprotein receptors (LDLR) causes familial hypercholesterolemia in humans, a disease characterized by elevated blood cholesterol concentrations, xanthomas, and coronary heart disease, providing compelling evidence that high blood cholesterol concentrations cause atherosclerosis. In this study, we used ^{1}H nuclear magnetic resonance spectroscopy to examine the metabolic profiles of plasma and urine from the LDLR knockout mice. Consistent with previous studies, these mice developed hypercholesterolemia and atherosclerosis when fed a high-fat/cholesterol/cholate-containing diet. In addition, multivariate statistical analysis of the metabolomic data highlighted significant differences in tricarboxylic acid cycle and fatty acid metabolism, as a result of high-fat/cholesterol diet feeding. Our metabolomic study also demonstrates that the effect of high-fat/cholesterol/cholate diet, LDLR gene deficiency, and the diet-genotype interaction caused a significant perturbation in choline metabolism, notably the choline oxidation pathway. Specifically, the loss in the LDLR caused a marked reduction in the urinary excretion of betaine and dimethylglycine, especially when the mice are fed a high-fat/cholesterol/cholate diet. Furthermore, as we demonstrate that these metabolic changes are comparable with those detected in ApoE knockout mice fed the same high-fat/cholesterol/cholate diet they may be useful for monitoring the onset of atherosclerosis across animal models.

atherosclerotic mouse model; hypercholesterolemia; metabolomics; systems biology; low-density lipoprotein; apolipoprotein E

ATHEROSCLEROSIS, A PROCESS involving progressive intimal thickening of the arterial wall, is the main cause of cardiovascular disease (14). It is often initiated by hypercholesterolemia and has been associated with both genetic and environmental risk factors (14, 30). While mice have become the most widely used animal model of atherosclerosis they are naturally resistant to this disease (10). However, the C57BL/6J strain is susceptible to diet-induced atherosclerosis (10), while the apolipoprotein E (apoE) and the low-density lipoprotein receptor (LDLR) gene deletion ($^{-/-}$) models develop large atherosclerotic lesions when fed a high-fat diet (2, 9). Indeed, ApoE$^{-/-}$ mice develop hypercholesterolemia and atherosclerosis even when fed normal rodent diet.

However, mutations of the apoE gene are rare in humans (30). In contrast, mutations in the LDLR gene are amongst the most prevalent genetic defects in humans (5). They cause familial hypercholesterolemia, a disease characterized by elevated blood cholesterol concentrations, xanthomas, and coronary heart disease (5). Small atherosclerotic lesions have been reported to develop in LDLR$^{-/-}$ mice fed a normal diet, but they develop severe atherosclerosis and large xanthomas when fed high-fat diet (9).

In humans, atherosclerotic cardiovascular disease has been associated with the metabolic syndrome, which includes insulin resistance, abdominal obesity, high blood pressure, low high-density lipoprotein cholesterol, and hypertriglyceridemia (reviewed in Refs. 19, 37). In addition to the conventional atherosclerotic risk factors, recent studies have suggested possible roles for other metabolites in the development and treatment of atherosclerosis. Homocysteine has been recognized as an independent risk factor of atherosclerosis (17), and betaine has been used to reduce blood homocysteine concentrations via the remethylation pathway (1, 28, 31). In addition, taurine supplementation is able to decrease serum cholesterol concentrations and retard arterial lipid accumulation in various animal models (11, 20, 21, 36).

In this study, we investigated the interaction between a high-fat/cholesterol/cholate (HFCC) diet and LDLR gene deficiency on plasma and urinary metabolic profiles in C57BL/6J mice using ^{1}H nuclear magnetic resonance (NMR) spectroscopy and multivariate statistics. This approach identified a profound metabolic perturbation in TCA cycle, fatty acid metabolism and a diet-genotype interaction in choline metabolism. We also analyzed the ^{1}H-NMR dataset by regression in association with the concentrations of plasma cholesterol and triglycerides and atherosclerotic lesion areas. Finally, a multivariate statistical model was used to analyze the data clustering of an independent ApoE$^{-/-}$ mouse dataset to examine metabolic differences that are common to both animal models.

Address for reprint requests and other correspondence: J. L. Griffin, Dept. of Biochemistry, Univ. of Cambridge, Hopkins Bldg., Tennis Court Rd., Cambridge CB2 1QW, UK (e-mail: jlg40@mole.bio.cam.ac.uk).

MATERIAL AND METHODS

Animals, diets, and experimental design. All procedures involving animals conformed to UK Home Office regulations and were approved by the Home Office. Fifteen-week-old female wild-type (C57BL/6J) and LDLR$^{-/-}$ (C57BL/6J background) mice were purchased from Jackson Laboratories (Bar Harbor, ME). Twenty-four mice from each strain were housed three per cage in a room that was lit from 6:00 AM to 6:00 PM and kept at 21°C. Two diets were used in this study: standard rodent diet (RM1; Special Diet Services, UK) and HFCC diet (Hope Farm, Woerden, the Netherlands) containing cocoa butter (15%), cholate (0.5%), cholesterol (1%), sucrose (40.5%), cornstarch (10%), corn oil (1%), cellulose (4.7%), casein (20%), choline chloride (1%), methionine (0.2%), and mineral mixture (5.1%).

A factorial design was used for this 18-wk study with two genotypes (C57BL/6J and LDLR$^{-/-}$ mice, $n = 24$) and two diets (RM1 and HFCC). Before the experiment, all 48 mice received food and water ad libitum and were fed RM1 diet for 3 wk. Then, 12 mice from each strain were weaned onto the HFCC diet for 12 wk. At *week 12*, three animals from each group were killed and the lesion areas were quantified histologically. The other 36 animals were then fed control RM1 diet for a further 6 wk to examine the return to normality for both mouse strains. At *week 18*, the remaining 36 animals were killed.

Urine (from each group of 3 animals in a cage collected for 24 h over dry ice) and plasma (from individual animals) were collected during the study (*week 0, 4, 8, 12* for urine; *week 8, 12,* and *18* for plasma) and analyzed by ^{1}H NMR spectroscopy at 500 MHz, using a solvent suppression pulse sequence based on a one-dimensional NOESY pulse sequence. Plasma total cholesterol and triglyceride concentrations were measured using kits (Wako Chemicals and Boehringer-Mannheim), respectively, and a 96-well plate reader (Thermomax, Molecular Devices, UK) with Softmaxpro software (version 2.4.1). Atherosclerotic lesion areas were measured in the aortic root of the mice at *week 12* (3 per group) and *week 18* (9 per group), where the mean lesion areas were calculated from 10 sections per mouse. Each section (stained with oil red O and hematoxylin) was imaged using an Olympus BH-2 light microscope and a Hitachi HV-C10 video camera and quantified using a PC (Datacell Pentium, P5–133; Datacell, Berks, UK) and Optimas image analysis software (version 6.1, Optimas) (7).

To cross-correlate metabolic changes across animal studies, in an independent study, female C57BL/6J and ApoE$^{-/-}$ mice (C57BL/6J background) ($n = 12$) were housed in groups of four and fed RM1 diet for 2 wk before the experiment. The ApoE$^{-/-}$ mice were weaned onto the HFCC diet for 12 wk, while the C57BL/6J mice continued to be fed RM1 diet. Urine samples taken at *weeks 0, 8,* and *12* were analyzed by ^{1}H NMR spectroscopy as in the LDLR$^{-/-}$ mouse study.

Data processing and statistical analysis. NMR spectra were processed using ACD SpecManager 1D NMR processor (version 8; ACD, Toronto, Canada). Spectra were Fourier transformed and referenced to sodium-3-(tri-methylsilyl)-2,2,3,3-tetradeuteriopropionate (Cambridge Isotope Laboratories, Andover, MA) at 0.0 ppm. Spectra were phased and baseline corrected manually. Each spectrum was integrated using 0.04 ppm integral regions between 0.2–4.45 and 5.15–10.0 ppm. To account for any difference in concentration between samples each spectral region was normalized to a total integral value of one for each spectrum. Datasets were imported into SIMCA-P+ 11.0 (Umetrics, Umeå, Sweden) for processing using principal components analysis (PCA), partial least squares (PLS) analysis, and PLS-discriminant analysis (PLS-DA, a regression extension of PCA used for classification). PLS-DA provides a graphical representation of the multivariate data, which is useful for class discrimination and prediction analysis in addition to identifying important metabolites that discriminate between different groups (as in univariate data analysis). The Q^2 and R^2 values from the resulting multivariate model were used to assess the robustness of a model, where R^2 shows the fraction of variation explained by a component and Q^2 shows the predictivity of the model through cross-validation. Typically, a robust model has a $Q^2 > 40\%$. In addition these models were assessed for robustness using the validation tool within SIMCA that assesses the Q^2 and R^2 for each model against models produced where the Y value for class membership has been permuted to produce random models. Here, a robust model is represented by Q^2 actual $>>$ Q^2 random.

The data were classified based on the diet and genotype: *class 1*, C57BL/6J mouse, RM1 diet; *class 2*, C57BL/6J mouse, HFCC diet; *class 3*, LDLR$^{-/-}$ mouse, RM1 diet; *class 4*, LDLR$^{-/-}$ mouse, HFCC diet; *class 5*, C57BL/6J mouse, RM1 diet, from ApoE$^{-/-}$ mouse study; *class 6*, ApoE$^{-/-}$ mouse, RM1 diet; and *class 7*, ApoE$^{-/-}$ mouse, HFCC diet. In the PCA and PLS-DA scores plots, the *week 18* data for *classes 2* and *4* were plotted as "2b" and "4b," respectively, to highlight the diet switch from *weeks 13* to *18*. Identification of major metabolic perturbations within the pattern recognition models was achieved by analysis of corresponding loadings plots. These were then confirmed by standard univariate tests (Student's *t*-test and ANOVA). For the NMR data, the *P* values shown were corrected with the Bonferroni correction unless otherwise specified. However, the univariate analyses of the clinical data (lesion area, total cholesterol, and total triglycerides concentrations) were not Bonferroni corrected. All NMR peaks were assigned based on the Human Metabolome database (34), published literature (22), and Chenomx NMR suite version 5.1 (Chenomx, Edmonton, Canada).

RESULTS

Diet, genotype, and their interaction cause severe perturbation in choline metabolism. Applying PLS-DA to the urinary ^{1}H-NMR dataset from the LDLR$^{-/-}$ study produced a model with eight components (Fig. 1*A*: $R^2X = 62\%$, $R^2Y = 56\%$, $Q^2 = 54\%$, for the first two components; Supplementary Fig. S1[1]: cross-validation plot for this model). The first PLS-DA component represented the data variation due to different diets. The corresponding metabolic changes are demonstrated in Fig. 1*B*, which shows the ^{1}H NMR spectra comparing C57BL/6J mice fed either the RM1 diet or the HFCC diet (NMR spectrum from an individual sample of each class; Supplementary Fig. S2A shows an NMR stack plot comparing both classes). For both C57BL/6J and LDLR$^{-/-}$ mice, the HFCC diet caused significant decreased urinary excretion of citrate (−66%, average difference based on integral area), α-ketoglutarate (−44%), succinate (−23%), taurine (−61%), hippurate (−74%), cis-aconitate (−32%), lactate (−22%), and urea (−48%), as well as increased concentrations of betaine (+388%), dimethylglycine (DMG, +71%), formate (+114%), and allantoin (+62%). Similar changes were found by repeating the analysis using the univariate two-way ANOVA (all $P < 0.001$). In addition, an increased concentration of trimethylamine (TMA, +44%) was observed, with an uncorrected *P* value of 0.0003. While the *P* value was adjusted to 0.068 following a Bonferroni correction, this is a conservative approach to false discovery.

The second PLS-DA component separated the LDLR$^{-/-}$ mice from the C57BL/6J mice. The corresponding PLS-DA loading characterizes the genotype discrimination with significant reduction of betaine (−70%), DMG (−44%), TMA (−28%), as well as an increased excretion of urea (+64%) for the LDLR$^{-/-}$ mice (all $P < 0.001$, except TMA, $P < 0.05$ according to subsequent ANOVA test; Fig. 1*C*, NMR spectrum from an individual sample of each class; Supplementary Fig.

[1] The online version of this article contains supplemental material.

S2B shows an NMR stack plot comparing both classes). Interestingly, ANOVA analysis also highlighted significant diet-genotype interaction for the urinary excretion of betaine, DMG, and cis-aconitate (all $P < 0.001$, Fig. 1*D*).

^{1}H-NMR analysis of plasma also demonstrated diet difference as the major source of metabolic variation. The PLS-DA of ^{1}H-NMR spectra of plasma data (excludes *week 18* data for *classes 2* and *4*; the 18 wk time point represents a period after

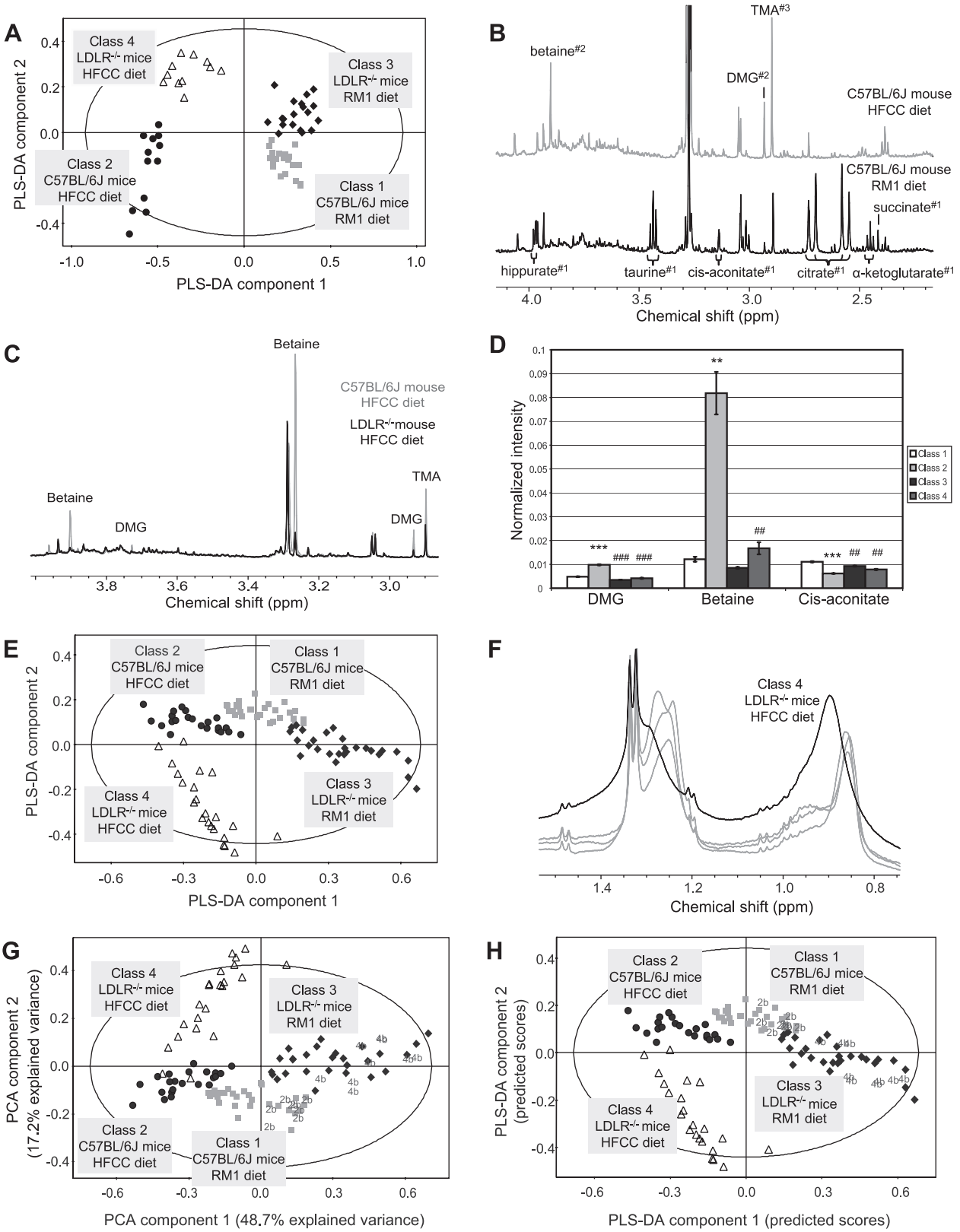

the animals had been fed the RM1 diet again) produced an eight-component model (Fig. 1*E*: $R^2X = 66\%$, $R^2Y = 53\%$, $Q^2 = 52\%$, for the first two components; Supplementary Fig. S3: cross-validation plot for this model). The discrimination of diet factor by the first component could be attributed to the significant reduction of fatty acid moieties (δ0.84, δ1.24–1.32, δ2.00, δ2.72–2.84, and δ5.27–5.35; 16–69% reduction across different resonances, NMR peak assignment in Table 1 and Supplementary Fig. S4), choline containing metabolites (δ3.20–3.24, consisting of resonances from choline, phosphocholine, and other choline-containing metabolites; −21%), as well as increased concentrations of betaine (+62%) and DMG (+41%) for the mice fed HFCC diet (all $P < 0.001$). In addition, the deficiency of LDLR was found to increase the concentrations of fatty acid moieties (δ0.84, δ0.88, δ1.28, δ2.00, δ2.76–2.84, and δ5.27–5.35, all $P < 0.001$; δ1.24, $P < 0.05$; P values obtained from subsequent ANOVA test; 11–61% increase in signal intensity in LDLR$^{-/-}$ mice compared with controls). The result of PLS-DA comparing the C57BL/6J and LDLR$^{-/-}$ mice fed the two different diets is summarized in Supplementary Table S1. Furthermore, the analysis of NMR spectra of plasma shows that the combined effect of both diet and genotype results in the lowest pool size of choline metabolites (δ3.20–3.24, $P < 0.001$), as well as a higher intensity of δ3.24–3.28 ($P < 0.001$, includes resonances from subclasses of choline metabolites, glucose, and betaine) for the *class 4* mice (LDLR/HFCC), compared with the three other classes. In addition, when the LDLR$^{-/-}$ mice were fed HFCC diet, a shift in the lipoprotein lipid resonances is observed. For this class of animals, the main lipoprotein lipid peaks shifted to 0.88–0.92 and 1.28–1.32 ppm, compared with 0.84–0.88 and 1.24–1.28 ppm for the three other classes (Fig. 1*F*). This most likely represents a change in the abundance of different lipoprotein subclasses in the plasma of *class 4* mice (LDLR/HFCC).

Analyzing the full plasma dataset with unsupervised PCA ($R^2X = 66\%$, $Q^2 = 63\%$ for the first two principal components) shows that the *week 18* data for mice previously fed HFCC diet but now on a normal diet ("2b," C57BL/6J mice; "4b," LDLR$^{-/-}$ mice; *week 1–12*, HFCC diet; *week 13–18*, RM1 diet; Fig. 1*G*) cluster with their counterparts fed RM1 diet throughout the study. This finding is consistent with a prediction analysis using the PLS-DA model shown in Fig. 1*E*, which classifies all "2b" samples as C57BL/6J mice fed RM1 diet, and "4b" samples as LDLR$^{-/-}$ mice fed RM1 diet (Fig. 1*H*).

Diet reverses hypercholesterolemia, but not atherosclerosis. Figure 2*A* summarizes the relative effect of HFCC diet and LDLR gene deficiency on atherosclerotic lesion areas and the concentrations of plasma cholesterol and triglycerides. The largest values for each category are normalized to 100 for comparison.

The mean atherosclerotic lesion areas for *classes 2–4* are significantly higher than *class 1* (C57/RM1) (*class 2*, C57/HFCC, 13-fold higher; *class 3*, LDLR/RM1, 25-fold higher; *class 4*, LDLR/HFCC, 241-fold higher). A reduction of atherosclerotic lesion area was not observed for *classes 2* and *4* by switching the HFCC diet to RM1 diet. There is a similar pattern between the class-mean of plasma cholesterol concentration (*week 12*) and the lesion area. At *week 12*, the cholesterol concentration of *class 4* (LDLR/HFCC) is 10-fold higher than *class 3* (LDLR/RM1). However, this effect of HFCC diet is reversible by refeeding the LDLR$^{-/-}$ mice the RM1 diet, and there is no significant difference in plasma cholesterol concentration for these two classes at *week 18* ($P = 0.84$, Student's *t*-test). Nevertheless, the plasma cholesterol concentrations for the LDLR$^{-/-}$ mice (*classes 3* and *4*) was significantly higher than the C57BL/6J mice (*classes 1* and *2*) at *week 18* when comparing the two mouse models regardless of diet ($P < 0.001$, Student's *t*-test).

Plasma triglyceride concentrations were found to be higher for LDLR$^{-/-}$ mice compared with C57BL/6J mice. Triglyceride concentrations were significantly lower when control mice were fed HFCC diet ($P = 1.8 * 10^{-5}$, Student's *t*-test), but no significant reduction was observed for the LDLR$^{-/-}$ mice ($P = 0.38$, Student's *t*-test). For all groups of animals, there was a significant increase in triglyceride concentrations at *week 18* compared with data from *week 12* ($P = 0.0006$–0.028, Student's *t*-test).

Applying PLS to explore associations between plasma metabolic profile and atherosclerotic lesion area for the *class 4* mice at *week 18* (LDLR/HFCC followed by RM1) produced a one-component model ($R^2Y = 81\%$, $R^2X = 47\%$, $Q^2 = 66\%$; Supplementary Fig. S5A: cross-validation plot for this model). A plot comparing predicted lesion area (from the PLS model) versus actual lesion area is shown in Fig. 2*B*. The corresponding loading plot indicated that the lesion area is negatively correlated with fatty acid moieties (δ1.28–1.32, δ1.56–1.60, and δ2.24–2.28). Nevertheless, it should be noted that the resultant model is not predictive for the other groups (data not shown). In addition, the same PLS analysis on each of *classes*

Fig. 1. *A*: partial least squares discriminant analysis (PLS-DA) scores plot showing clustering of urinary ^{1}H-nuclear magnetic resonance (NMR) dataset for the low-density lipoprotein receptor deletion (LDLR$^{-/-}$) study ($R^2X = 62\%$, $R^2Y = 56\%$, and $Q^2 = 54\%$ for the first 2 PLS-DA components). *B*: section of ^{1}H-NMR spectra (δ2.2–4.0) showing major urinary metabolic changes corresponding to diet difference (NMR spectrum from an individual sample of each class). #1Significantly higher concentration for mice fed standard rodent (RM1) diet; #2significantly higher concentration for mice fed high-fat-cholesterol with cholate (HFCC) diet; #3higher concentration for mice fed HFCC diet across both strains ($P = 0.0676$). DMG, dimethylglycine; TMA, trimethylamine. *C*: ^{1}H-NMR spectra (δ2.9–4.0) showing significant reduction in urinary concentrations of choline derivatives as a result of LDLR deficiency (betaine, $P < 0.001$; DMG, $P < 0.001$; TMA, $P < 0.05$; across both diets) (NMR spectrum from an individual sample of each class). *D*: column plot showing normalized peak intensity of urinary DMG, betaine, and cis-aconitate. Error bars represent standard error. *Class 1*, C57BL/6J mouse, RM1 diet; *class 2*, C57BL/6J mouse, HFCC diet; *class 3*, LDLR$^{-/-}$ mouse, RM1 diet; *class 4*, LDLR$^{-/-}$ mouse, HFCC diet. *P* values were obtained by comparing each genotype on different diets (*$P < 0.05$, **$P < 0.01$, ***$P < 0.001$) and by comparing different genotypes fed the same diet (#$P < 0.05$, ##$P < 0.01$, ###$P < 0.001$). *E*: PLS-DA scores plot showing clustering of plasma ^{1}H-NMR data from the LDLR$^{-/-}$ study ($R^2X = 66\%$, $R^2Y = 53\%$, and $Q^2 = 52\%$ for the first 2 PLS-DA components). *Week 18* data for *classes 2* and *4* were excluded from this analysis. *F*: a shift in the lipoprotein lipids resonance (δ0.84–0.92 and δ1.24–1.32) in the plasma NMR spectrum is observed for the *class 4* mice (black spectrum), compared with the 3 other classes (grey spectra). *G*: principal components analysis (PCA) scores plot for plasma ^{1}H-NMR dataset for the LDLR$^{-/-}$ study ($R^2X = 66\%$, and $Q^2 = 63\%$ for the first 2 principal components), showing clustering for *week 18* data of *class 2* (symbol, 2b; C57BL/6J mice; *week 0–12*, HFCC diet; *week 13–18*, RM1 diet) and *class 4* (symbol, 4b; LDLR$^{-/-}$ mice; *week 0–12*, HFCC diet; *week 13–18*, RM1 diet). *H*: PLS-DA scores plot showing the projection of *week 18* data for *class 2* (2b) and *class 4* (4b) onto the PLS-DA model in *E*. The model predicts samples 2b as the C57BL/6J mice fed RM1 diet and samples 4b as the LDLR$^{-/-}$ mice fed RM1 diet.

Table 1. *^{1}H NMR resonance assignments for plasma in the LDLR$^{-/-}$ study (22)*

Chemical Shift, ppm	Peak Assignment
0.84–0.88	lipid (mainly LDL): $CH_3(CH_2)_n$
0.88–0.92	lipid (mainly VLDL): $CH_3CH_2CH_2C=$
1.24–1.28	lipid (mainly LDL): $(CH_2)_n$ lipid: $CH_3CH_2(CH_2)_n$
1.28–1.32	lipid (mainly VLDL): $CH_2CH_2CH_2CO$ lipid: CH_2
1.56–1.60	lipid (mainly VLDL): CH_2CH_2CO
2.00–2.04	lipid: $CH_2C=C$
2.24-2.28	lipid: CH_2CO
2.72–2.84	lipids: $C=CCH_2C=C$
2.93	dimethylglycine (DMG)
3.20–3.24	choline metabolites
3.27, 3.90	betaine
5.27–5.35	unsaturated lipids

NMR, nuclear magnetic resonance; LDLR, low-density lipoprotein receptor.

1–3 at *week 12* produced unsatisfactory models (*classes 2* and *3*, no model; *class 1*, one PLS component; $R^2 = 43\%$ for linear regression model comparing predicted and actual lesion area). Furthermore, the application of PLS to correlate the plasma metabolome with lesion data for all animals produced a distinct two clusters, which separates *class 4* animals (with substantially larger lesion area than other classes) from the rest of the animals (data not shown).

On the other hand, PLS analysis correlating both the total cholesterol and total triglycerides concentrations with lesion area for *class 4* mice at *week 18* produced an unsatisfactory model demonstrating that the metabolomic profile was much more predictive of lesion area compared with classical clinical chemistry measures ($R^2Y = 59\%$, $R^2X = 43\%$, $Q^2 = 21\%$, one PLS component; Supplementary Fig. S5B: cross validation plot for this model; Supplementary Fig. S6: a plot comparing predicted lesion area vs. actual lesion area for this model).

PLS-DA model of the LDLR$^{-/-}$ mouse dataset as a predictive model for the ApoE$^{-/-}$ mice. The PLS-DA model from Fig. 1*A* was used to predict the data clustering for the independent ApoE$^{-/-}$ mouse dataset. All of the C57BL/6J mice fed RM1 diet were correctly predicted as *class 1* (labeled "5," Fig. 3*A*). One out of three samples of ApoE$^{-/-}$ mice fed RM1 diet (labeled "6," Fig. 3*A*) is predicted as *class 1* with the other two samples adjacent to *class 1* (Fig. 3*A*).

The class "7" samples (ApoE/HFCC) are clustered adjacent to the *class 4* mice (LDLR/HFCC) in the prediction model. The multivariate statistics showed that unlike the C57BL/6J mice, both the ApoE$^{-/-}$ and the LDLR$^{-/-}$ mice did not respond to the HFCC diet with increased urinary concentrations of betaine and DMG. Figure 3*B* shows a Cooman's plot comparing ApoE$^{-/-}$ mice with C57BL/6J (*class 2*) and LDLR$^{-/-}$ mice (*class 4*), all fed HFCC diet. The SIMCA model classifies ApoE$^{-/-}$ mice ("7") as outliers that do not belong to either *class 2* or *4*. The main difference between the ApoE$^{-/-}$ mice compared with the two other genotypes is that the excretion of the TCA cycle intermediates for the ApoE$^{-/-}$ mice remains unchanged when the mice were challenged with the HFCC diet. By including only betaine, DMG, and TMA in the SIMCA analysis (Fig. 3*C*), the model predicted five out of six of the "7" samples (ApoE/HFCC) in the model space of *class 4* (LDLR/HFCC). This result indicated that the APOE$^{-/-}$ mice had the same perturbation in choline metabolism in response to the HFCC diet, similar to the LDLR$^{-/-}$ mice. Thus, while the LDLR$^{-/-}$ and ApoE$^{-/-}$ mice have distinct metabolic profiles some changes associated with the response to HFCC diet are consistent across the studies.

DISCUSSION

HFCC diet and deficiency of the LDLR gene both caused significant metabolic perturbation in the plasma and urinary profiles of the C57BL/6J mice (strain background for both transgenic mouse models used in the study), in addition to previously reported hypercholesterolemia and atherosclerosis (9, 10). Our metabolomic study demonstrated that the HFCC diet caused a dramatic decrease in the urinary taurine excretion of all of the mice (C57BL/6J, LDLR$^{-/-}$ and ApoE$^{-/-}$). Our data, taken together with previous findings, indicate a possible metabolic role of taurine in the development of atherosclerosis in mice. Indeed, it is known that the C57BL/6J strain has a defect in taurine renal reabsorption that causes them to excrete more taurine than other mouse strains (26). C57BL/6J mice are reported to be more susceptible to diet-induced atherosclerosis

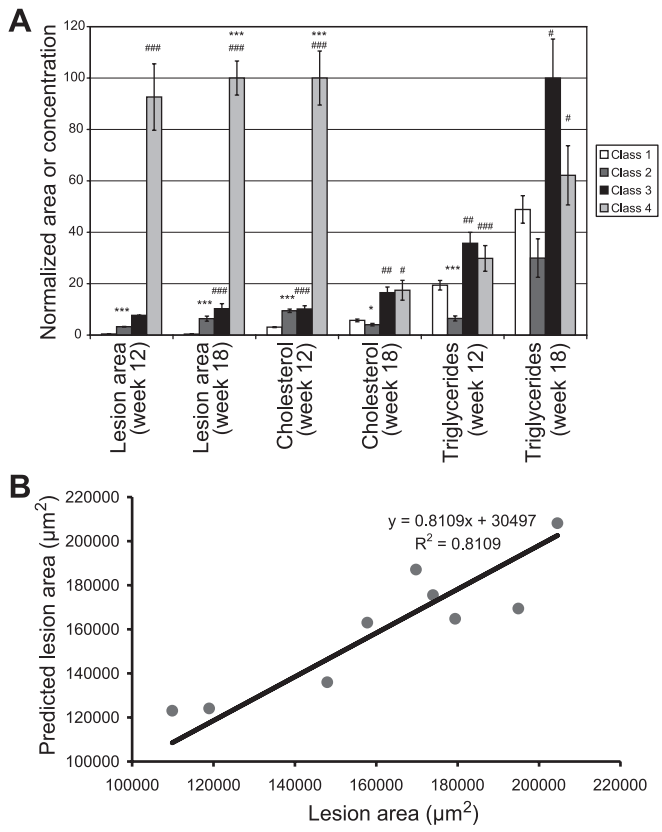

Fig. 2. *A*: column plot comparing the atherosclerotic lesion areas and concentrations of plasma cholesterol and triglycerides at *weeks 12* and *18*. The largest values for each category were normalized to 100 for comparison. Error bars represent standard error. *Class 1*, C57BL/6J mouse, RM1 diet; *class 2*, C57BL/6J mouse, HFCC diet; *class 3*, LDLR$^{-/-}$ mouse, RM1 diet; *class 4*, LDLR$^{-/-}$ mouse, HFCC diet. *P* values were obtained by comparing each genotype fed different diets ($*P < 0.05$, $**P < 0.01$, $***P < 0.001$) and by comparing different genotypes fed the same diet ($\#P < 0.05$, $\#\#P < 0.01$, $\#\#\#P < 0.001$). *B*: predicted lesion area vs. actual lesion area using PLS model correlating plasma NMR data with the lesion area for *class 4* animals at *week 18* ("4b," 1 PLS component; $R^2X = 47\%$, $R^2Y = 81\%$, $Q^2 = 66\%$).

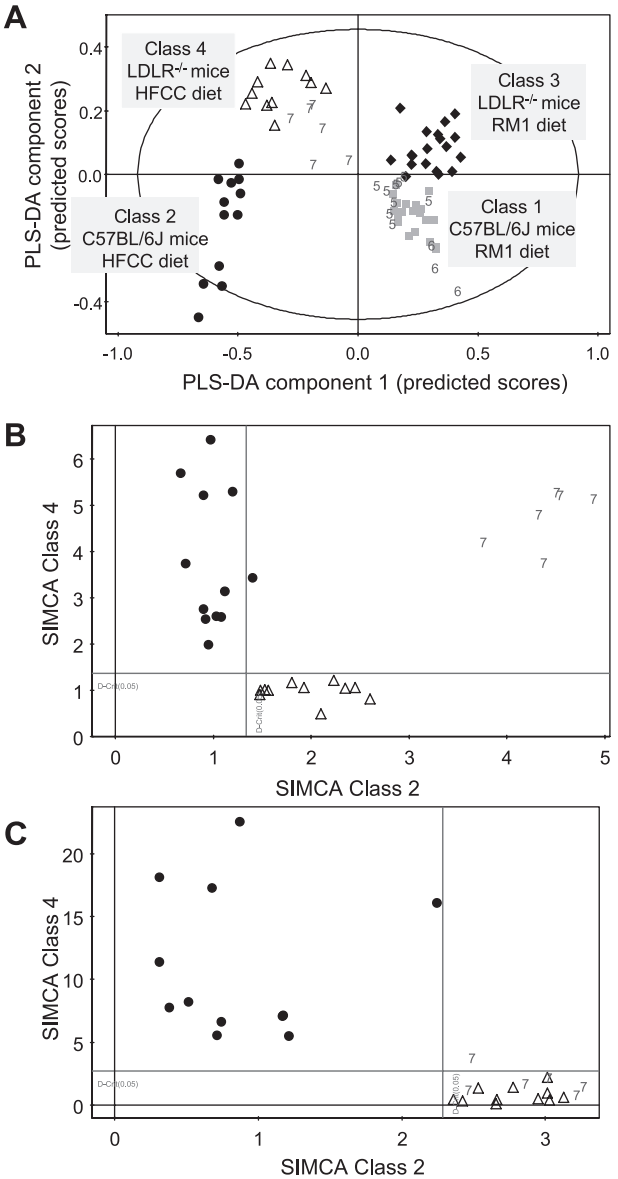

Fig. 3. *A*: prediction model for an independent apolipoprotein E deletion ($ApoE^{-/-}$) mouse dataset using the PLS-DA model in Fig. 1*A*. Definitions: 5, C57BL/6J mice, RM1 diet; 6, $ApoE^{-/-}$ mice, RM1 diet; 7, $ApoE^{-/-}$ mice, HFCC diet. *B*: Cooman's plot comparing C57BL/6J (*class 2*, ●), $LDLR^{-/-}$ (*class 4*, △) and $ApoE^{-/-}$ (symbol, 7) mice fed HFCC diet. The SIMCA model classifies "7" samples as outliers, which fell outside of the model space of *class 2* and *4*. *C*: Cooman's plot comparing C57BL/6J (*class 2*), $LDLR^{-/-}$ (*class 4*) and $ApoE^{-/-}$ ("7") mice fed HFCC diet. By including only betaine, DMG, and TMA in the SIMCA analysis, 5 out of 6 of the "7" samples fell into the model space of *class 4*.

than other strains of mice (10). Furthermore, taurine supplementation was reported to decrease serum cholesterol, increase cholesterol 7α-hydroxylase activity, and retard arterial lipid accumulation in C57BL/6J mice (20). Interestingly, in humans, a strong and inverse association between taurine excretion and mortality from ischemic heart disease was reported previously (35). A study in Japanese Okinawan immigrants living in Brazil (i.e., with high meat and low fish intake) showed a lower taurine excretion but a higher mortality rate from coronary heart disease compared with the founder population in Okinawa (18). Feeding HFCC diet in the present study caused a substantial decrease in taurine excretion in both the control and $LDLR^{-/-}$ mice, suggesting either that there was less taurine in the diet or that taurine was being consumed by other processes, upstream of the kidney, e.g., for conjugation with the added cholate in the HFCC diet and subsequent loss by bacterial metabolism in the intestine. Secretion of taurine or glycine conjugated bile acids in bile, and incomplete reabsorption in the ileum is one of the two major mechanisms by which cholesterol is lost from the body, secretion of biliary free cholesterol being the other (6). It has also been reported that Wistar rats fed a high-cholesterol diet had a marked reduction of taurine in serum, liver, kidney, and heart, accompanied with increased hepatic cholesterol 7α-hydroxylase activity and fecal bile acid and cholesterol (36).

In previous metabolomics investigations, a reduction in the urinary concentration of TCA cycle intermediates has been associated with dietary differences, hepatotoxicity, and vascular lesions (reviewed in Ref. 25). In both C57BL/6J and $LDLR^{-/-}$ mice, significant reductions in the urinary concentrations of TCA cycle intermediates (citrate, α-ketoglutarate, succinate, and cis-aconitate) were observed when the mice were fed HFCC diet. Surprisingly, similar changes were not found when the $ApoE^{-/-}$ mice were fed the same diet. Unfortunately, with the NMR analysis of plasma, the comparison of the concentrations of TCA cycle intermediates between groups is not straightforward due to their relatively low peak intensity, and their co-resonance with larger lipids peaks, but it seems likely that similar changes would occur in plasma.

The concentrations of cholesterol and triglycerides in plasma have been recognized as risk factors of atherosclerosis. The result from both ^{1}H-NMR spectroscopy and biochemical assay showed that the mice fed HFCC diet had lower plasma triglyceride concentrations, despite a significant increase in plasma cholesterol concentrations. This has previously been suggested to be due to the combined effects of cholesterol and cholate in the HFCC diet (33). However, the reduction of plasma triglycerides concentration below the concentration of mice fed RM1 diet did not protect either C57BL/6J or $LDLR^{-/-}$ mice from atherosclerosis when they were fed HFCC diet. Furthermore, at *week 18*, the plasma cholesterol concentrations did not correlate well with the atherosclerotic lesion area ($r = 0.47$, Pearson's correlation coefficient). This suggests that plasma cholesterol is heavily influenced by diet and therefore is not a good indicator for the severity of atherosclerosis in the present study.

Reis and colleagues (24) previously reported that pre-existing atherosclerotic lesions were dramatically reduced (~76% reduction) 9 wk after the transplantation of aortae from the $ApoE^{-/-}$ mice (fed a Western diet for 38 wk) into C57BL/6J mice fed normal diet. In another study by Ramachandran and colleagues (23), aortic lesions were reduced by ~35% by switching the $LDLR^{-/-}$ mice previously fed high-fat diet for 3 mo to a normal rodent diet for another 3 mo. From the same study, even greater reductions were observed if normal rodent diet was accompanied by exercise. Our present results show that no regression of pre-existing lesions was evident after switching HFCC-diet fed $LDLR^{-/-}$ mice to RM1 diet for 6 wk. Nevertheless, it should be noted that the ratio of regression phase (6 wk) to diet-induction phase (12 wk) for the present study is 50% lower than the Ramachandran study, suggesting that the time postswitch may have been too short to see a reduction.

Multivariate statistics indicated that when LDLR$^{-/-}$ mice fed HFCC diet (*class 4*) for 12 wk were switched to RM1 diet for a further 6 wk their plasma profiles clustered with the LDLR$^{-/-}$ mice fed RM1 diet for 18 wk, indicating that the metabolic profiles converged reasonably rapidly after the change of diet. Despite this change of profile, application of PLS analysis produced a robust multivariate model that correlated the plasma metabolic profile with the atherosclerotic lesion areas. This suggests that there are markers associated with lesion area that are detectable despite a change of diet, especially fatty acid moieties, which deserve further investigation. In addition, our PLS analysis also showed that this plasma NMR data correlate better with lesion areas than did total cholesterol and total triglycerides concentrations measured in the clinical chemistry screen. However, intriguingly the model developed based on NMR data was not predictive for the other study groups. This might be due to substantial difference in lesion area between samples used for model development (*class 4* mice at *week 18*) and samples in the prediction set. Although the result of this study does not fully explain the finding, it suggests that the metabolic state of the plasma in the atherosclerotic animal might provide useful insights into which factors determine atherosclerotic plaque area in the regression phase of atherosclerosis.

The two ^{1}H-NMR studies revealed a significant perturbation in choline metabolism (Fig. 4) as a result of different diets, genotypes, and their interaction. Choline can be obtained from diet or by de novo synthesis of phosphatidylcholine from phosphatidylethanolamine (27, 38). Some of the known biological functions of choline and its metabolites include ensuring the structural integrity of cell membranes and lipoproteins, cell signaling, cholinergic neurotransmission, lipid transport, and as a major source of methyl groups for methylation reactions (39). Choline deficiency has been associated with fatty liver, liver damage, lymphocyte apoptosis, and DNA damage (4, 38).

Although the present findings do not offer a full explanation for the large differences in choline metabolism, several hypotheses can be advanced for further investigation. It is known that failure to express the LDLR results in delayed LDL clearance and, consequently, hypercholesterolemia and atherosclerosis (5). However, the metabolic impact of a possible low recycling rate of choline-containing metabolites (the building block of lipoprotein) to the liver is rarely discussed. Our results suggest that the oxidation of choline to betaine and subsequently DMG is markedly reduced in LDLR knockout mice, but upregulated by feeding HFCC diet. Hypercholesterolemia or LDLR deficiency might cause a higher consumption of choline for further lipoprotein synthesis. In the case where LDLR$^{-/-}$ mice were placed on HFCC diet, our result suggests a possible change in the abundance of different subclasses of lipoproteins, as signified by the change in line shape for the CH_3- and -$CH_2CH_2CH_2$-lipid envelopes (13, 32), and choline metabolites in the plasma of hypercholesterolemic LDLR$^{-/-}$ mice.

Li and Vance (12) showed that the oxidation of choline to betaine is strikingly reduced during choline deprivation. However, in our study, the plasma and urinary betaine concentrations cannot be explained solely by choline availability because betaine and DMG concentrations in plasma and urine from mice fed RM1 diet were lower than in their counterparts fed HFCC diet, despite the former maintaining a larger pool of choline-containing metabolites in their plasma. In humans, the known physiological role of betaine is as an organic osmolyte and as a methyl donor to methylate homocysteine to methionine in liver and kidneys (3). Importantly, betaine supplementation is reported to attenuate atherosclerogenesis in ApoE$^{-/-}$ mice (15). In animal models, it also reduces plasma homocysteine concentrations (29), a known atherosclerotic risk factor that is associated with enhanced vascular inflammation and oxidative stress (8, 16).

In conclusion, our metabolomic study shows that the HFCC diet and LDLR gene deficiency caused a significant metabolic perturbation in the TCA cycle, fatty acid metabolism, and choline metabolism. Our results demonstrate that the loss of LDLRs caused a marked reduction in the urinary excretion of betaine and DMG. We postulate that the delayed LDL clearance due to LDLR deficiency results in a lower recycling rate of choline-containing metabolites. This, together with a higher

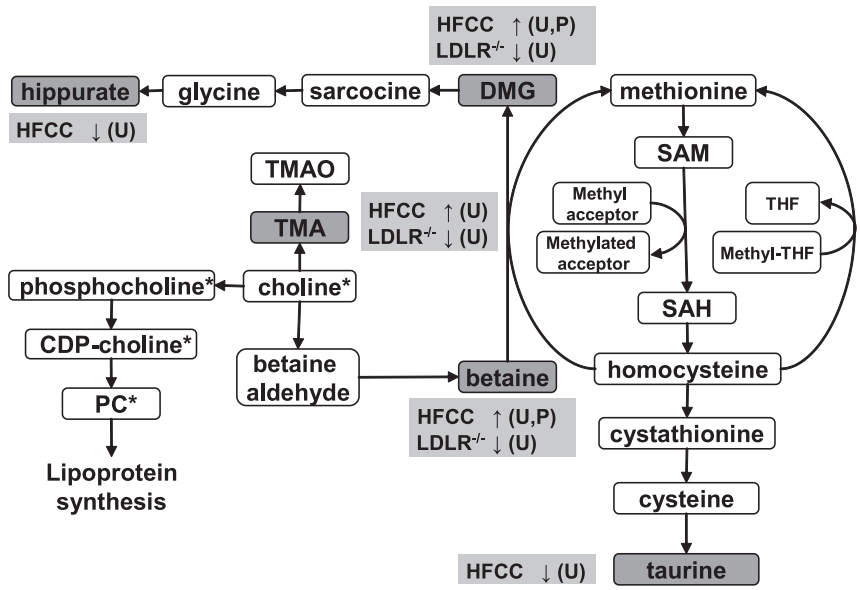

Fig. 4. Choline metabolism is perturbed by HFCC diet, LDLR deficiency, and the interaction between both main factors. PC, phosphatidylcholine; SAH, S-adenosylhomocysteine; SAM, S-adenosylmethionine; THF, tetrahydrofolate; TMAO, trimethylamine oxide. The relative changes in plasma (P) and urine (U) as a result of HFCC diet and LDLR deficiency are shown with arrows (↓, decreased; ↑, increased). *HFCC diet caused a significant reduction in choline metabolites in plasma (δ3.20–3.24, which includes resonance from choline, phosphocholine, and other choline-containing metabolites).

choline consumption for lipoprotein synthesis, caused a significant perturbation in choline metabolism, notably the choline oxidation pathway in the $LDLR^{-/-}$ mice.

GRANTS

The authors gratefully thank the support from Universiti Teknologi Malaysia (K. K. Cheng) and the Royal Society, UK (J. L. Griffin).

DISCLOSURES

No conflicts of interest are declared by the authors.

REFERENCES

1. **Atkinson W, Elmslie J, Lever M, Chambers ST, George PM.** Dietary and supplementary betaine: acute effects on plasma betaine and homocysteine concentrations under standard and postmethionine load conditions in healthy male subjects. *Am J Clin Nutr* 87: 577–585, 2008.
2. **Breslow JL.** Mouse models of atherosclerosis. *Science* 272: 685–688, 1996.
3. **Craig SA.** Betaine in human nutrition. *Am J Clin Nutr* 80: 539–549, 2004.
4. **Da Costa KA, Niculescu MD, Craciunescu CN, Fischer LM, Zeisel SH.** Choline deficiency increases lymphocyte apoptosis and DNA damage in humans. *Am J Clin Nutr* 84: 88–94, 2006.
5. **Goldstein JL, Brown Familial hypercholesterolemia MS.** Lipoprotein and lipid metabolism disorders. In: *The Metabolic Basis of Inherited Disease*, edited by Scriver CR, Beaudet AL, Sly WS, and Valle D. New York: McGraw-Hill, 1989, p. 1215–1250.
6. **Hansen SH.** The role of taurine in diabetes and the development of diabetic complications. *Diabetes Metab Res Rev* 17: 330–346, 2001.
7. **Hockings P, Roberts T, Galloway G, Reid D, Harris D, Vidgeon-Hart M, Groot P, Suckling K, Benson G.** Repeated three-dimensional magnetic resonance imaging of atherosclerosis development in innominate arteries of low-density lipoprotein receptor-knockout mice. *Circulation* 106: 1716, 2002.
8. **Hofmann MA, Lalla E, Lu Y, Gleason MR, Wolf BM, Tanji N, Ferran LJ Jr, Kohl B, Rao V, Kisiel W, Stern DM, Schmidt AM.** Hyperhomocysteinemia enhances vascular inflammation and accelerates atherosclerosis in a murine model. *J Clin Invest* 107: 675–683, 2001.
9. **Ishibashi S, Goldstein JL, Brown MS, Herz J, Burns DK.** Massive xanthomatosis and atherosclerosis in cholesterol-fed low density lipoprotein receptor-negative mice. *J Clin Invest* 93: 1885–1893, 1994.
10. **Jawien J, Nastalek P, Korbut R.** Mouse models of experimental atherosclerosis. *J Physiol Pharmacol* 55: 503–517, 2004.
11. **Kondo Y, Toda Y, Kitajima H, Oda H, Nagate T, Kameo K, Murakami S.** Taurine inhibits development of atherosclerotic lesions in apolipoprotein E-deficient mice. *Clin Exp Pharmacol Physiol* 28: 809–815, 2001.
12. **Li Z, Vance DE.** Phosphatidylcholine and choline homeostasis. *J Lipid Res* 49: 1187–1194, 2008.
13. **Lounila J, Ala-Korpela M, Jokisaari J, Savolainen MJ, Kesäniemi YA.** Effects of orientational order and particle size on the NMR line positions of lipoproteins. *Phys Rev Lett* 72: 4049–4052, 1994.
14. **Lusis AJ.** Atherosclerosis. *Nature* 407: 233–241, 2000.
15. **Lv S, Fan R, Du Y, Hou M, Tang Z, Ling W, Zhu H.** Betaine supplementation attenuates atherosclerotic lesion in apolipoprotein E-deficient mice. *Eur J Nutr* 48: 205–212, 2009.
16. **Matte C, Stefanello FM, Mackedanz V, Pederzolli CD, Lamers ML, Dutra-Filho CS, Dos Santos MF, Wyse AT.** Homocysteine induces oxidative stress, inflammatory infiltration, fibrosis and reduces glycogen/glycoprotein content in liver of rats. *Int J Dev Neurosci* 27: 337–344, 2009.
17. **McCully KS.** Homocysteine and vascular disease. *Nat Med* 2: 386–389, 1996.
18. **Mizushima S, Moriguchi EH, Nakada Y, Biosca MDG, Nara Y, Murakami K, Horie R, Moriguchi Y, Mimura G, Yamori Y.** The relationship of dietary factors to cardiovascular diseases among Japanese in Okinawa and Japanese immigrants, originally from Okinawa, in Brazil. *Hypertens Res* 15: 45–55, 1992.
19. **Moller D, Kaufman K.** Metabolic syndrome: a clinical and molecular perspective. *Annu Rev Med* 56: 45–62, 2005.
20. **Murakami S, Kondo-Ohta Y, Tomisawa K.** Improvement in cholesterol metabolism in mice given chronic treatment of taurine and fed a high-fat diet. *Life Sci* 64: 83–91, 1999.
21. **Murakami S, Nara Y, Yamori Y.** Taurine accelerates the regression of hypercholesterolemia in stroke-prone spontaneously hypertensive rats. *Life Sci* 58: 1643–1651, 1996.
22. **Nicholson JK, Foxall PJ, Spraul M, Farrant RD, Lindon JC.** 750 MHz 1H and 1H-13C NMR spectroscopy of human blood plasma. *Anal Chem* 67: 793–811, 1995.
23. **Ramachandran S, Penumetcha M, Merchant NK, Santanam N, Rong R, Parthasarathy S.** Exercise reduces preexisting atherosclerotic lesions in LDL receptor knock out mice. *Atherosclerosis* 178: 33–38, 2005.
24. **Reis ED, Li J, Fayad ZA, Rong JX, Hansoty D, Aguinaldo JG, Fallon JT, Fisher EA.** Dramatic remodeling of advanced atherosclerotic plaques of the apolipoprotein E-deficient mouse in a novel transplantation model. *J Vasc Surg* 34: 541–547, 2001.
25. **Robertson DG, Lindon JC, Nicholson JK, Holmes E.** *Metabonomics in Toxicity Assessment*. Boca Raton, FL: Taylor & Francis, 2005.
26. **Rozen R, Scriver CR, Mohyuddin F.** Hypertaurinuria in the C57BL/6J mouse: altered transport at the renal basolateral membrane. *Am J Physiol Renal Fluid Electrolyte Physiol* 244: F150–F155, 1983.
27. **Sanders LM, Zeisel SH.** Choline: dietary requirements and role in brain development. *Nutr Today* 42: 181–186, 2007.
28. **Schwab U, Torronen A, Toppinen L, Alfthan G, Saarinen M, Aro A, Uusitupa M.** Betaine supplementation decreases plasma homocysteine concentrations but does not affect body weight, body composition, or resting energy expenditure in human subjects. *Am J Clin Nutr* 76: 961–967, 2002.
29. **Schwahn BC, Wang XL, Mikael LG, Wu Q, Cohn J, Jiang H, Maclean KN, Rozen R.** Betaine supplementation improves the atherogenic risk factor profile in a transgenic mouse model of hyperhomocysteinemia. *Atherosclerosis* 195: e100–e107, 2007.
30. **Smith JD, Breslow JL.** The emergence of mouse models of atherosclerosis and their relevance to clinical research. *J Intern Med* 242: 99–109, 1997.
31. **Steenge GR, Verhoef P, Katan MB.** Betaine supplementation lowers plasma homocysteine in healthy men and women. *J Nutr* 133: 1291–1295, 2003.
32. **Suna T, Salminen A, Soininen P, Laatikainen R, Ingman P, Mäkelä S, Savolainen MJ, Hannuksela ML, Jauhiainen M, Taskinen MR, Kaski K, Ala-Korpela M.** 1H NMR metabonomics of plasma lipoprotein subclasses: elucidation of metabolic clustering by self-organising maps. *NMR Biomed* 20: 658–672, 2007.
33. **Vergnes L, Phan J, Strauss M, Tafuri S, Reue K.** Cholesterol and cholate components of an atherogenic diet induce distinct stages of hepatic inflammatory gene expression. *J Biol Chem* 278: 42774–42784, 2003.
34. **Wishart D, Tzur D, Knox C, Eisner R, Guo A, Young N, Cheng D, Jewell K, Arndt D, Sawhney S.** HMDB: the human metabolome database. *Nucl Acids Res* 35: D521, 2007.
35. **Yamori Y, Liu L, Ikeda K, Miura A, Mizushima S, Miki T, Nara Y.** Distribution of twenty-four hour urinary taurine excretion and association with ischemic heart disease mortality in 24 populations of 16 countries: results from the WHO-CARDIAC study. *Hypertens Res* 24: 453–457, 2001.
36. **Yokogoshi H, Mochizuki H, Nanami K, Hida Y, Miyachi F, Oda H.** Dietary taurine enhances cholesterol degradation and reduces serum and liver cholesterol concentrations in rats fed a high-cholesterol diet. *J Nutr* 129: 1705–1712, 1999.
37. **Zambon A, Pauletto P, Crepaldi G.** the metabolic syndrome-a chronic cardiovascular inflammatory condition. *Aliment Pharmacol Ther Suppl* 22: 20, 2005.
38. **Zeisel SH.** Choline: critical role during fetal development and dietary requirements in adults. *Annu Rev Nutr* 26: 229–250, 2006.
39. **Zeisel SH, Blusztajn JK.** Choline and human nutrition. *Annu Rev Nutr* 14: 269–296, 1994.